

Research Article

Obtaining TiO₂ Nanostructures by Electrospinning and Analysis of Absorbance in the UVA Spectrum for Photocatalytic Application

Luana Góes Soares^{*}, Annelise AlvesUniversidade Federal do Rio Grande do Sul (UFRGS), Avenida Osvaldo Aranha, sala 709, CEP 90035-190, Porto Alegre-RS, Brazil; E-Mails: lugoes.soares@gmail.com; annelise.alves@ufrgs.br^{*} **Correspondence:** Luana Góes Soares; E-Mail: lugoes.soares@gmail.com**Academic Editor:** Ermelinda Falletta**Special Issue:** [Recent Advances in TiO₂ Photocatalysis and Applications](#)*Catalysis Research*

2023, volume 3, issue 2

doi:10.21926/cr.2302016

Received: December 14, 2022**Accepted:** April 10, 2023**Published:** April 17, 2023

Abstract

The synthesis of fibers by electrospinning allows for obtaining nanostructures of one-dimensional materials with good flexibility, optical and catalytic properties, high surface area and porosity. They can be used in applications such as: catalysts, solar cells, fuel cells, membranes, and hydrogen batteries, among others. Here we emphasize that few reports in the literature describe the existing synergism between the optical and photocatalytic properties of TiO₂, and the influence of this synergism on the formation of oxygen vacancies, which are responsible for the increase of the photocatalytic activity of this photocatalyst. Therefore, in this work we synthesize TiO₂ nanofibers by electrospinning. These nanofibers were thermally treated between 650°C and 800°C, and characterized according to: morphology by scanning electron microscopy (SEM), crystalline phases by X-ray diffraction (XRD), photoactivity through degradation tests of 125 mL of a sample of 20 ppm methyl orange dye solution and by colorimetry. The results point to the TiO₂ sample heat-treated at 650°C being more effective in the dye degradation and the reflection of different colors, possibly due to the combination of the chemical and physical properties of TiO₂, which at the same time degrade the dye and express variations between different colors.



© 2023 by the author. This is an open access article distributed under the conditions of the [Creative Commons by Attribution License](#), which permits unrestricted use, distribution, and reproduction in any medium or format, provided the original work is correctly cited.

Keywords

TiO₂; electrospinning; absorbance; colors; photocatalysis

1. Introduction

It was in the 1970s that the production of ceramic fibers with diameters in the range of micrometers for commercial applications began. The initial studies involved the development of technologies that generate fibers from non-oxide materials based on Si-C, later materials with stoichiometry similar to this material were tested, however due to limitations regarding its oxidative capacity, since it cannot be used in an oxidizing atmosphere and not at high temperatures, stimulated studies using fibers made of ceramic oxides [1].

This method produces fibers with significant characteristics such as variable diameters from submicrometric to nanometric, high surface area, porosity, and permeability, among other properties. It is based on using electrostatic forces, where solvents with medium dielectric properties are used. When electrostatic forces overcome the surface tension of the polymeric solution, a polymeric liquid jet begins to be launched toward the collector [1]. Currently, producing fibers/nanofibers by electrospinning has been studied extensively, and several polymeric solutions can be prepared for producing fibers/nanofibers through this technique [2].

Among nanomaterials, fibers are the one-dimensional nanostructures that have attracted the most attention, due to their flexibility, being anisotropic, and generating great interaction with other areas of science, such as: material sciences, biology, physics, chemistry, medical areas, among others [1]. Some main applications include: photocatalytic degradation of dyes [2-4], antimicrobial action [2], and preservation of food packaging [2], among others.

Due to global demand and aiming at sustainability, more and more attention is focused on preserving the environment. Water contamination and consequently the treatment and final destination of water resources is one issue that has challenged scholars, who suggest preventing and controlling water pollution as an inevitable trend, aiming at sustainable development. Therefore, obtaining a catalyst that can effectively decontaminate organic pollutants from water would be a huge advance [5]. And it is within this context that since the 70s, photocatalytic processes have been successfully used in the degradation of organic compounds, treatment of effluents, etc. TiO₂, as the most commonly used semiconductor, in heterogeneous photocatalysis, acquires relevance, due to its efficiency in the decomposition of pollutants in water, air, bacteria, and cancer cells and the degradation of toxic organic compounds. Se apresenta sob três formas polimórficas, a anatase, brookita e rutilo. Among these phases, anatase seems to have the highest photocatalytic activity. It is preferred among semiconductors, as it has the following characteristics: non-toxicity, insolubility in water, photostability, the possibility of immobilization on solids and chemical stability in a wide range of pH [1].

Studies prove a synchrony between the optical and photocatalytic properties of titanium oxide (TiO₂). In 2018, researchers from the Federal University of Rio Grande did Sul [1] observed that photochromism and photocatalysis are phenomena that are correlated through the occurrence of similar effects, since at the same time that they alter the optical properties of the material, they also degrade the orange dye of methyl. This verified synchrony occurs because the chemistry and

physics of this oxide (TiO_2), when optically activated, are similar. Because during optical and photocatalytic activation, the valence band electrons, occupied only by the 2p orbitals of O, are promoted to the conduction band, forming electron/hole pairs (e^-/h^+). The Ti^{3+} sites capture the electrons that are promoted to the conduction band, causing the reduction of the ions. The holes, conversely, can dissociate H_2O molecules or organic proton donor molecules, which are adsorbed on the surface of the particles, generating positively charged O_2 holes, which capture the photoexcited electrons. The presence of active oxygen vacancy centers has attracted much attention due to their significant improvement in the responsiveness to visible light, and inhibiting the recombination of the electron/hole pair.

Thus, as an agent of scientific dissemination, this research has the scope to contemplate the theme of natural resources, about the construction of sustainable application mechanisms. Therefore, TiO_2 fibers were produced by electrospinning in order to relate the optical and photocatalytic properties of these samples. Aiming through the result of heterogeneous photocatalysis and heterogeneous photocatalysis tests in the UVA region, suggest its application in the treatment of effluents. Therefore, few studies are reporting the existing synergism between the optical and photocatalytic properties of TiO_2 , and its influence on the generation of oxygen vacancies.

2. Materials and Methods

For the execution of this work, the steps described below were carried out.

2.1 Sample Preparation

The fibers were obtained by preparing TiO_2 precursor solutions, containing a mixture of 2.5 mL of titanium isopropoxide (TIP), 2.0 mL of glacial acetic acid and 5.0 mL of an alcoholic solution containing 10% by weight of polyvinylpyrrolidone (PVP), as shown in Figure 1.



Figure 1 Precursor solution for the production of fibers by electrospinning.

2.1.1 Electrospinning

Then, a plastic syringe loaded with 5 mL of the TiO₂ precursor solution was connected to a stainless-steel needle, powered by a high-voltage source. The distance between the capillary and the cylindrical collector was 12 cm, the applied voltage was 13.5 kV and the flow of 1.8 ml/h. The cylindrical collector was covered with aluminum foil to collect the nanofibers produced every 30 minutes for 4 hours daily. After electrospinning synthesis, the nanofibers were heat treated in an electric oven (SANCHIS) at 650°C, 700°C, 750°C or 800°C with a 1 h hold and a heating rate of 1.4°C/min.

2.2 Characterization of Samples Obtained by Electrospinning

A PHILIPS diffractometer with CuK α radiation was used, with a voltage of 40 kV and 40 mA, equipped with the X'PERT HighScore[®] software, to identify the phases present in the fibers. The morphology of the samples was observed using scanning and transmission electron microscopy (SEM and TEM) techniques. The equipment used was an SEM, JEOL JSM 6060) and a TEM, JEOL JEM 1200ExII. The diameter of the TiO₂ fibers was measured using the UTHSCSA ImageTool[®] program. Ten measurements were made for each fiber before heat treatment and after treatment at 650°C, 700°C, 750°C and 800°C. After the measurements, the average of the fibers was taken at each corresponding temperature, thus obtaining the value of the average diameter of the TiO₂ fibers. Fiber thickness was observed using an Ambios XP2 Technology profilometer. The equipment used to measure band gap energy was a spectrophotometer dual-beam UV-vis-NIR (Cary 5000), with an integrating sphere in reflection mode diffused light. The band gap energy values were obtained through the Kubelka correlation and Munk. The photocatalytic performance of TiO₂ nanofibers was analyzed by changing the concentration of the methyl orange dye under UVA irradiation. The photocatalysis process was carried out in a pyrex glass photocatalytic reactor, where the radiation was provided by 12 black UVA lamps, 8 W each, model Fluor BLB T5 and Sadokin brand. The lamps are arranged in two semi-cylinders, which have reflective inner surfaces. The other components of the photocatalytic reactor include; a magnetic stirrer, a compressed air aeration system and a thermostatic bath. In carrying out the photocatalytic assays, the TiO₂ nanofibers were mixed with 125 mL of a solution containing 20 ppm of the methyl orange dye. The mixture was placed in an ultrasound (Cole-Parmer CP-750) for 15 minutes. The solution was then transferred to the photocatalytic reactor, under constant stirring, and at a temperature of 30°C. Air bubbles during the period of exposure to UVA light. Before each trial, a sample of 4 mL of this solution was collected and defined as the initial sample. During the test, with the UVA light system turned on, 4 mL aliquots of the solution, at 15-minute intervals, were filtered through 0.2 μ m filters and placed in polymethylmethacrylate (PMMA) to then be analyzed by spectrophotometry. The colorimetric analyzes were carried out using a Konica Minolta 2600 spectrophotometer, which uses the i7[®] software, which comes with the equipment, and records the data using the color scale of the CIE-Lab system. In this system, color is registered as a coordinate in a 3-axis system, with a* (red and green) and b* (yellow and blue) axes varying between positive and negative values, and L* (luminescence) varying between 0 to 100%. Negative a* values represent green influence, and positive a* values represent red influence. Negative b* values represent the blue influence and positive b* values represent the yellow influence. On the L* axis, 0% represents black (no reflected light) and 100% represents white (total reflection).

3. Results

3.1 Morphological Analysis of Samples

Figure 2 (a-b) shows the scanning electron microscopy (SEM) images of the surface of TiO₂ fibers heat treated at 650°C and 800°C, respectively. From the images, it can be seen that the TiO₂ fibers appear to have a morphology consisting of an agglomerate of primary particles, randomly dispersed, with an elongated and continuous format and without a preferred orientation. The TEM images in Figure 3 (a-b), ratifying the images in Figure 2 (a-b), reveal that TiO₂ fibers consist of a set of interconnected particles or crystals, showing the presence of small grains [1].

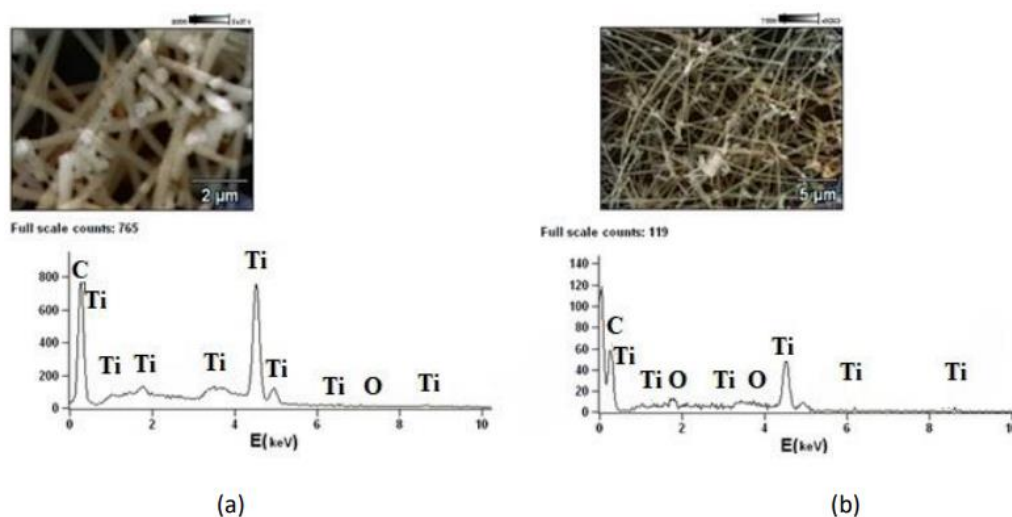


Figure 2 SEM image of the TiO₂ sample, heat treated at (a) 650°C and (b) 800°C, respectively.

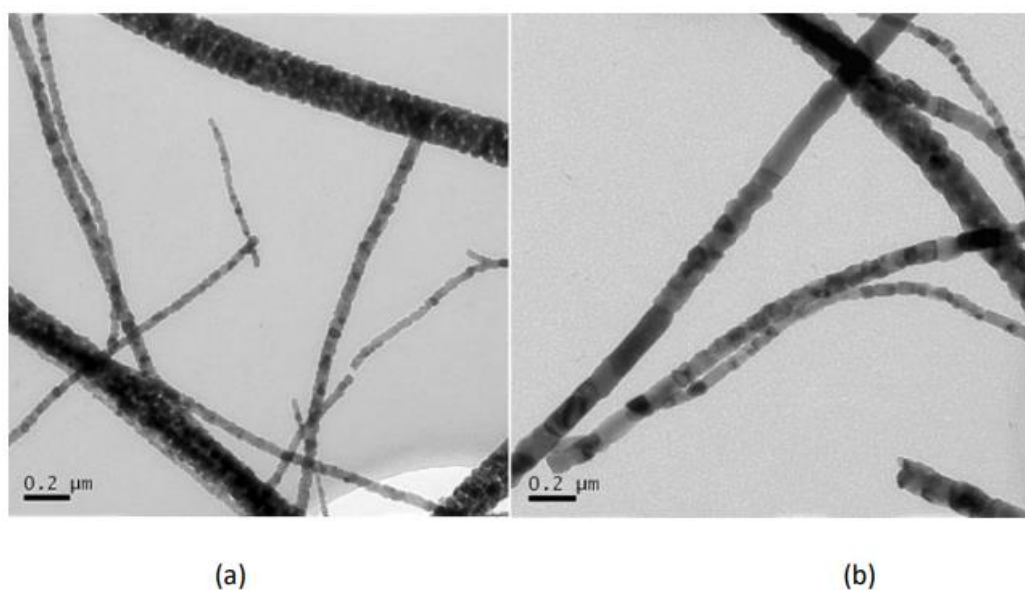


Figure 3 TEM image of the TiO₂ sample, heat treated at (a) 650°C and (b) 800°C, respectively.

Table 1 presents the relationship between the heat treatment conditions and the diameter of the TiO₂ fibers. These results were obtained using the UTHSCSA Image Tool® program, already mentioned in the manuscript's methodology. It is observed that with the increase in the heat treatment temperature, the diameter of the fibers, originally 0.35 μm, suffers a gradual reduction up to 0.16 μm. This phenomenon can be attributed to the loss by combustion of polymeric compounds initially present in the fibers and possibly to their sintering [1]. Table 1 also presents the thickness values of the TiO₂ fibers. In general, the thickness positively influenced the colorimetric and photocatalytic performance of the fibers. Favoring the photocatalytic performance and the fibers' reflectance of the different colors.

Table 1 Diameter and thickness of fibers obtained by electrospinning.

Fibers	Diameter(μm)	Thickness (μm)
WHT	0.35	3.19
650°C	0.34	3.06
700°C	0.25	3.05
750°C	0.19	3.04
800°C	0.16	3.02

Figure 4 shows the diffractogram of fibers synthesized by electrospinning. The samples before heat treatment were amorphous. It can be seen that the diffractogram of the sample without heat treatment (WHT) is typical for amorphous material, which proves the need for heat treatment to order the atoms in the crystal and obtain a crystalline phase. Furthermore, the higher the calcination temperature, the more defined the peaks, which shows an increase in the material's crystallinity. The first characteristic peak of the anatase phase was observed at a temperature of 650°C, at approximately 25.156° with a Miller index (101). For the TiO₂ fibers treated up to a temperature of 700°C, only the presence of the anatase crystalline phase (JCPDS 010782486) was identified, with the first characteristic peak at approximately $2\theta = 25.271^\circ$. Fibers treated from 750°C onwards presented, in addition to the anatase phase, the rutile phase (JCPDS 01-077-0442), que corresponded to Miller index (110), with the first characteristic peak at approximately $2\theta = 27.294^\circ$, resulting from the occurrence of a TiO₂ phase transition, predicted after increasing the heat treatment temperature [6]. The heat treatment temperature influenced the proportion of the anatase and rutile phases present in the TiO₂ fibers, as predicted by the literature [6, 7], and presented in Table 2. The measurements were performed using the X'PERT HighScore® software that accompanies the diffractometer. Fibers heat treated at 650°C and 700°C, presented the formation of 100% of the anatase crystalline phase, above this temperature, at 750°C and 800°C, there was the formation of 50% and 70%, respectively, of the rutile phase. This phenomenon is expected, as the rutile phase is the stable phase of titanium oxide. Increasing temperature promotes the, transformation of metastable structures, such as anatase into rutile [1, 7].

Table 2 Anatase/rutile proportion present in TiO₂ fibers obtained by electrospinning.

Fibers	% Anatase	% Rutile
WHT	-	-
650°C	100	-

700°C	100	-
750°C	50	50
800°C	30	70
P25 (standard)	78.36	21.63

Table 3 Colorimetric records of the samples.

Samples	a*	b*	L%	Hue difference (light/dark) ΔL*	Absorbed color
Fibers 650°C	+1.47	-12.51	83.33	-35.99	Dark-blue
Fibers 700°C	+3.29	-2.68	61.42	-57.43	Dark-blue
Fibers 750°C	+7.16	-10.44	92.14	-24.32	Dark-blue
Fibers 800°C	+4.14	-8.21	86.76	-42.86	Dark-blue
P25	+6.45	-2.23	83.13	-32.21	Dark-blue

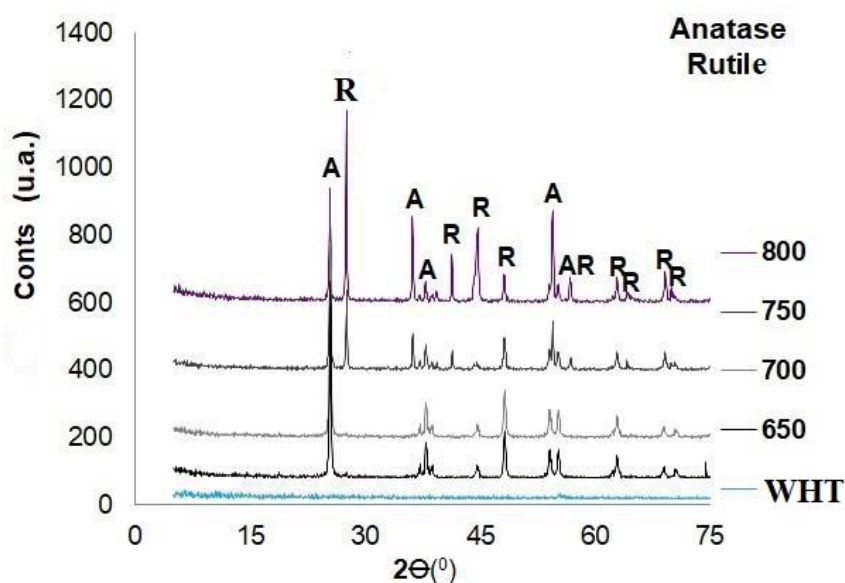


Figure 4 Diffractogram of TiO₂ fibers.

Figure 5 shows the catalytic activity of TiO₂ fibers in the degradation of methyl orange dye during 150 minutes of exposure to UV-A light ($\lambda = 365$ nm). The photodegradation capacity of the samples was compared to the commercial powder P25 Degusa, which was used as a reference. The most effective TiO₂ samples in the degradation of the methyl orange dye were those subjected to heat treatment at 650°C and 700°C, respectively, because it contains in its structures the majority presence of the anatase phase, which is proven to be the most photoactive phase of TiO₂ [7].

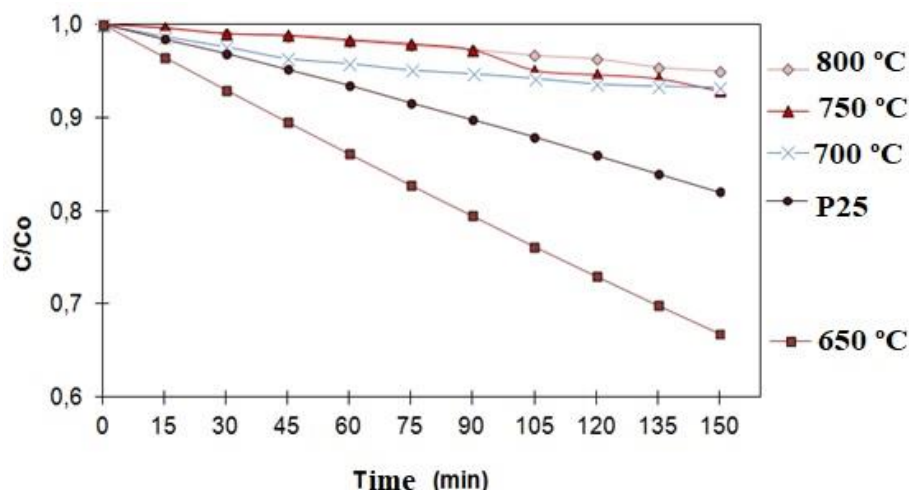


Figure 5 Photocatalytic activity of TiO₂ and P25 fibers.

The decrease observed in the photoactivity of the samples heat treated at 750°C and 800°C results from the formation of the rutile phase, which in the case of the fibers appears from 750°C. The rutile form is less photoactive than the anatase form, so its appearance reduces the photocatalytic activity of the synthesized fibers. Another reason, which explains this drop in the photocatalytic activity of the samples, is the fact that rutile is a semiconductor with a direct band gap. At the same time, the anatase phase is indirect, which causes the photogenerated carriers to recombine more quickly in the rutile phase than in the anatase phase [1, 7].

These observations were also described by Kocijan *et al.*, 2022 [8]. Where the dye concentration decreased with irradiation time in the presence of the investigated catalysts, this suggests that the photon energies, the smallest gap, and the formed phase are very important, influencing the photoactivity of the samples to degrade organic compounds.

3.2 Analysis Colorimetric

The results of the colorimetric tests carried out on the P25 standard and the TiO₂ fibers are presented in Table 3. The records for each sample were obtained based on the CIE-L*a*b* system, and the measurement range covers the entire visible spectrum (400 to 700 nm). Table 3 also presents the luminescence values (%L), the amount of light perceived in a given color. If the luminescence (%L) is close to 0%, it represents the total absence of reflected light (black) and if it is close to 100%, it represents the total reflection of light (white) [9]. And the ΔL^* values, inform about the differences between shades in lighter or darker. Positive (+) ΔL^* values indicate lighter color and negative (-) ΔL^* values indicate darker color.

Thus, during the colorimetric tests, the P25 standard and the TiO₂ fibers had maximum absorbance in the dark blue region, influenced by positive a* values (red color) and negative b* values (blue color). The dark hue of the samples was determined based on negative ΔL^* values. The maximum absorbance in the blue color region (440-485 nm) reached by the TiO₂ fibers was already expected, since the precursor solution prepared for producing fibers by electrospinning (Figure 1) has a yellow color. And, in colorimetric analysis, the maximum absorbance of material occurs in the region of the complementary color and, in this case, the complementary color to yellow is blue. The

P25 standard and the TiO₂ fibers had a good amount of perceived light, according to the luminescence values (%L) shown in Table 3.

3.3 Performance Analysis in the UVA Spectrum

The band gap values of the TiO₂ fibers and the P25 standard are presented in Table 4. These values are important because they make the distinction between semiconductor oxides and insulators, which are determined based on the occupation of the energy bands. Table 4 shows the fiber band gap reduction as the calcination temperature increases. This increase in temperature favors: the optical properties of the material and the surface effects on the distribution of electronic levels, increasing the light absorption capacity [7, 9]. In intrinsic semiconductors, as in the case of the fibers synthesized in this work, the band gap energy (E_g) is characterized by a filled valence band and an empty conduction band. It is through the thermal or optical excitation of the electrons that the formation of the energy gap in the valence band occurs, and the electrons are promoted to the conduction band. With the increase in temperature, there is a reduction in the band gap of the fibers in addition to the generation of disorder in their electronic structure, favoring the optical properties of the material [7, 10].

Table 4 Band gap values and their respective wavelength of fibers produced by electrospinning.

Samples	Band gap (eV)	λ (nm)
Fibers 650°C	2.80	442
Fibers 700°C	2.79	444
Fibers 750°C	2.78	446
Fibers 800°C	2.77	447
P25	2.81	441

All samples produced absorbed light at wavelengths between 440 and 485 nm, that is, in the blue color region of the electromagnetic spectrum. The energy of the molecule increases with the radiation absorbed by the photon. Visible and ultraviolet light cause the transfer of electrons to orbitals of higher energy and, in the ultraviolet, chemical bonds that ionize molecules still occur. According to Table 4, the samples are in the 2.77 to 2.81 eV range, respectively. The values obtained by our samples indicate that they can be used as semiconductors in heterogeneous photocatalysis, as the band gap values indicate that they are semiconductor materials with good optical properties.

4. Discussion

The obtained results were possible, due to the existing correlation between the optical and photocatalytic properties, which are phenomena that are correlated through the occurrence of similar effects, because at the same time that it modifies the color of the material, it also degrades the methyl orange dye. Below are some phenomena that occur simultaneously during photocatalysis and colorimetric tests, and they explain how it was possible to obtain the results above. Are they:

- (a) Electromagnetic radiation, usually UV, is essential to activate the material optically and photocatalytically. This radiation needs to overcome the band gap of the material in question, resulting in the formation of electron/hole pairs [7];
- (b) Need for the existence of a specific wavelength, which needs to be equal to or less than that determined by the Planck equation, which will provide the energy that will excite the material in question in the case of photocatalysis and reflect a certain color in the case of photochromism [7];
- (c) Migration of electrons from the valence band to the conduction band, generating positive holes (electron holes) in the valence band, when irradiated with light at an energy level higher than the band gap of the samples, which will degrade the dye and reflect/will absorb light, modifying the color of the material. In colorimetry, electrons from the valence band, occupied only by the 2p orbitals of O, are promoted to the conduction band, occupied by the 5d orbitals of W, forming electron/hole pairs (e^-/h^+). The W^{6+} sites capture the electrons that are promoted to the conduction band, causing the reduction of the ions. The holes, can dissociate H_2O molecules or organic molecules that donate protons, which are adsorbed on the surface of the particles [8]. The reflection/absorption of light modifies the color of the material, generating positively charged O_2 gaps that capture the photoexcited electrons [11]. In photocatalysis, when the irradiated light reaches an energy level higher than the band gap, electrons move from the valence band to the conduction band and simultaneously generate positive electron holes in the valence band.

5. Conclusions

The obtained results prove that the optical and photocatalytic properties are phenomena that are correlated through the occurrence of similar effects. At the same time that they modify the material's color, they also degrade the methyl orange dye. In both events, the irradiated light, the band gap energy and the wavelength were essential for the visual perception of the different colors and the photoactivity in the degradation of the methyl orange dye. All fibers can be used as photocatalysts and in colorimetric tests. Even the TiO_2 fibers treated at higher temperatures (750°C and 800°C), which showed low photoactivity, could degrade the methyl orange dye and absorb the color. Based on the obtained results, we suggest the application of these fibers in the treatment of effluents and the degradation of organic dyes.

Acknowledgments

This work was carried out with the support of the National Council for Scientific and Technological Development (CNPq), a Brazilian government entity focused on training human resources. The authors also thank the financial support of Brazilian agencies: Coordination for the Improvement of Higher Education Personnel (CAPES) and Research Support Foundation of the State of Rio Grande do Sul (FAPERGS).

Author Contributions

All authors contributed equally to the realization of this work.

Competing Interests

The authors have declared that no competing interests exist.

References

1. Soares L, Alves A. Photocatalytic properties of TiO₂ and TiO₂/WO₃ films applied as semiconductors in heterogeneous photocatalysis. *Mater Lett*. 2018; 211: 339-342.
2. Chougule SS, Gurme ST, Jadhav JP, Dongale TD, Tiwari AP. Low density polyethylene films incorporated with Biosynthesised silver nanoparticles using *Moringa oleifera* plant extract for antimicrobial, food packaging, and photocatalytic degradation application. *J Plant Biochem Biotechnol*. 2021; 30: 208-214.
3. Yadav NG, Chaudhary LS, Sakhare PA, Dongale TD, Patil PS, Sheikh AD. Impact of collected sunlight on ZnFe₂O₄ nanoparticles for photocatalytic application. *J Colloid Interface Sci*. 2018; 527: 289-297.
4. Kadam SJ, More KV, Chavan SS, Dongale TD, Shendekar SM. Electrospun 1D TiO₂ nanofibers for dye-sensitized solar cell application. *Mater Today*. 2022; 65: 106-110.
5. Nagamine S, Matsumoto T, Hikima Y, Ohshima M. Fabrication of porous carbon nanofibers by phosphate-assisted carbonization of electrospun poly (vinyl alcohol) nanofibers. *Mater Res Bull*. 2016; 79: 8-13.
6. Zhang LY, Yang JJ, Han YL. Novel adsorption-photocatalysis integrated bismuth tungstate modified layered mesoporous titanium dioxide (Bi₂WO₆/LM-TiO₂) composites. *Opt Mater*. 2022; 130: 112581.
7. Feltrin J, Sartor MN, Bernardin AM, Hotza D, Labrincha JA. Superfícies fotocatalíticas de titânia em substratos cerâmicos: Parte I: Síntese, estrutura e fotoatividade. *Cerâmica*. 2013; 59: 620-632.
8. Kocijan M, Vukšić M, Kurtjak M, Ćurković L, Vengust D, Podlogar M. TiO₂-based heterostructure containing *g*-C₃N₄ for an effective photocatalytic treatment of a textile dye. *Catalysts*. 2022; 12: 1554.
9. Soares L, Alves A. Analysis of colorimetry using the CIE-L*a*b* system and the photocatalytic activity of photochromic films. *Mater Res Bull*. 2018; 105: 318-321.
10. von Bezold JFW. Ueber das gesetz der farbenmischung und die physiologischen grundfarben. *Ann Phys*. 1873; 226: 221-247.
11. Sobrinho JA. Fotocromismo e luminescência de compostos a base de tungstênio e íons terras raras trivalentes via síntese hidrotérmica. Araraquara: Universidade Estadual Paulista; 2015.